

PRESSURE AND PRESSURE DERIVATIVE ANALYSIS IN A RESERVOIR WITH A FINITE-CONDUCTIVITY FAULT AND CONTRAST OF MOBILITIES

Freddy Humberto Escobar¹, Javier Andrés Martínez² and Matilde Montealegre Madero³

ABSTRACT

Finite-conductivity faults present a very unique transient behavior. In general terms, as the fault is reached by the pressure disturbance the pressure derivative falls with forming a straight line with a slope of minus one, then bilinear flow takes place which is reflected by a quarter-slope seen on the pressure derivative curve. At much later time, the radial flow regime is reached again.

In this work, the signature of the pressure derivative curve for the reservoirs with finite-conductivity faults is investigated to understand their behavior and facilitate the interpretation of well test data. This paper presents the most complete analytical well pressure analysis methodology for finite-conductivity faulted systems when a mobility contrast, using some characteristics features found on the pressure and pressure derivative log-log plot. Hence, new equations are introduced to estimate the fault conductivity for such systems. The proposed expressions and methodology were successfully tested with synthetic cases.

Key words: *Radial flow, bilinear flow, fault conductivity, steady state, mobility ratio*

ANÁLISIS DE PRESION Y DERIVADA DE PRESIÓN EN UN YACIMIENTO CON UNA FALLA DE CONDUCTIVIDAD FINITA Y CONTRASTE DE MOVILIDADES

RESUMEN

Las fallas con conductividad finita presentan un comportamiento único transitorio. En términos generales, a medida que la falla es alcanzada por la perturbación la derivada de presión cae formando una recta con pendiente de menos uno, luego toma lugar el flujo bilineal reflejado con una pendiente de un cuarto en la curva de la derivada de presión. A tiempos mucho más tardíos se alcanza nuevamente el flujo radial.

En este trabajo se investiga la huella de la derivada de presión en yacimientos que contienen fallas de conductividad finita para entender su comportamiento y facilitar la interpretación de pruebas de presión. Este artículo presenta la metodología analítica de pruebas de presión más completa para sistemas fallados con conductividad finita cuando hay un contraste de movilidades, usando ciertas características halladas en el gráfico logarítmico de la derivada de presión. De aquí que se introducen nuevas ecuaciones para determinar la conductividad de la falla para los sistemas en consideración. Las expresiones y metodología propuestas se verificaron satisfactoriamente con ejemplos sintéticos.

Palabras claves: *Flujo radial, flujo bilineal, conductividad de falla, estado estable, relación de movilidad*

1. Ph.D., Universidad Surcolombiana/CENIGAA. Neiva. Colombia. E-mail: fescobar@usco.edu.co

2. B.Sc., Universidad Surcolombiana. Neiva. Colombia. E-mail: jandres@usco.edu.co

3. M.Sc., Universidad Surcolombiana/CENIGAA. Neiva. Colombia. E-mail: matildelina2005@hotmail.com

INTRODUCTION

Many hydrocarbon-bearing formations are faulted and often little information is available about the actual physical characteristics of such faults. Some faults are known to be sealing and some others are non-sealing to the migration of hydrocarbons. While sealing faults block fluid and pressure communication with other regions of the reservoir, infinite-conductivity faults act as pressure support sources and allow fluid transfer across and along the faults planes. Finite-conductivity faults fall between these two limiting cases of sealing and totally non-sealing faults, and are believed to be included in the majority of faulted systems.

A sealing fault is often generated when the throw of the fault plane is such that a permeable stratum on one side of the fault plane is completely juxtaposed against an impermeable stratum on the other side. On the contrary, a non-sealing fault usually has an insufficient throw to cause a complete separation of productive strata on opposite sides of the fault plane. Depending on the permeability of the fault, fluid flow may occur along the fault within the fault plane or just across it laterally from one stratum to another. In general, a finite-conductivity fault exhibits a combined behavior of flow along and across its plane.

Pressure transient analysis offers a possible way to determine the fluid transmissibility of faults. Many models introduced in the literature help characterize faults from pressure transient tests. The simplest of such models uses the well-known method of images for sealing faults. This approach results in doubling the slope of the straight line on a semilog plot of pressure test data. Extensions to intersecting or no intersecting multiple sealing faults have also been reported in the literature. A finite-conductivity fault displays a one-fourth slope on the pressure derivative plot which is equivalent to be identified as a straight line in the Cartesian plot of pressure versus the one-fourth root of time. This behavior was reported by Trocchio [1] who conducted a study on the Fateh Mishrif reservoir and provided a conventional methodology for determining fracture conductivity and fracture length.

Cinco-Ley, Samaniego and Dominguez [2] considered the infinite-conductivity fault (or fracture) case and derived an analytical solution for pressure transient behavior using the concept of source functions. They also provided a type-curve matching interpretation

methodology. The first attempt to represent a fault as a partial barrier was introduced by Stewart, Gupta and Westaway [3] who numerically modeled the fault zone as a vertical-semi-permeable barrier of negligible capacity. This model correctly imposed the linear flow pattern at the fault plane. They found for interference tests that in cases where the conventional method cannot be applied, the inverse problem (non-linear regression analysis) was an excellent approach. Yaxely [4] derived analytical solutions for partially communicating faults by generalizing the approach presented by Bixel, Larkin, and van Poolen [5] for reservoirs with a semi-impermeable linear discontinuity. The generated type curves by their solutions yielded separate estimations of the formation transmissibility and the fault transmissibility. Ambastha, McLeroy and Grader [6] analytically modeled partially communicating faults as a thin skin region in the reservoir according to the concepts of skin presented by van Everdingen [7] and Hurst [8]. They concluded that for moderate skin values, the pressure response departs from the line-source solution, follows the double-slope behavior for some time, and then reverts back to a semilog linear pressure response parallel to the line-source solution at late time.

The models considered by Stewart et al. [3], Yaxely [4], and Ambastha et al. [6] allow for fluid transfer only laterally across the fault planes. These models do not account for fluid flow along the fault plane which can take place when the permeability of the fault plane is larger than the reservoir permeability surrounding it. A recent model proposed by Boussila, Tiab and Owayed [9] considers dual porosity behavior in a composite system. All these models neglected the fluid conductance inside the fault along its planes. However, Abbaszadeh and Cinco-Ley [10] modeled a finite-conductivity fault by specifying the fault parameters with the longitudinal fluid conductance (F_{CD}) and transverse skin factor (s_F). These authors neglected the transient nature in the fault zone. They provided some type curves for interference pressure test interpretation.

Anisur Rahman, Miller and Mattar [11] presented an analytical solution in the Laplace space to the transient flow problem of a well located near a finite-conductivity fault in a two-zone, composite reservoir. Contrary to previous studies, this solution also considered flow within the fault. They verified their solution by comparing a number of its special cases with those reported in the literature.

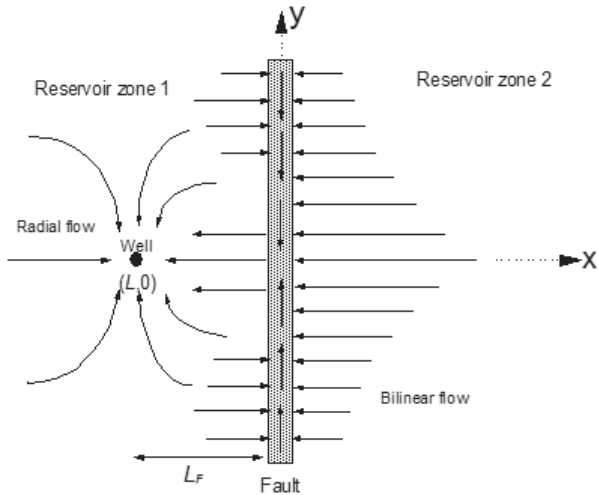


Figure 1. Schematic a finite-conductivity fault displaying the streamlines, after Anisur Raman et al. [11]

Escobar, Martínez and Montealegre-Madero [12] used the model introduced by Anisur Raman et al. [11] to successfully develop a well-test interpretation methodology which uses characteristic points found on the pressure and pressure derivative (*TDS* technique) for the case of unit mobility contrast. Conventional straight-line methodology was also complemented. The goal of the present work is to extend the interpretation methodologies (*TDS* and conventional analysis) for the case of different mobility contrast.

1. PRESSURE BEHAVIOR OF FINITE-CONDUCTIVITY FAULTS

In the finite-conductivity fault model used by Anisur Rahman et al. [11], the fault permeability is larger than the reservoir permeability. Fluid flow is allowed to occur both across and along the fault plane, and the fault enhances the drainage capacity of the reservoir. A schematic of the system is given in Figure 1. In their original solution, Abbaszadeh and Cinco-Ley [10] allowed a change of mobility and storativity in the two reservoir regions. In this study, only it is assumed a change of mobility.

When properties of reservoir at two side of the fault plane are not the same, complexities in addition to fault conductivity and skin effects are introduced. Figure 2 and 3 generated for finite-conductivity faults show dimensionless pressure derivative curves at several dimensionless fault conductivity and mobility ratios.

At Mobility ratios greater than one, the minimum point increases and increases as the mobility ratio, the distance between the curves for the same conductivity decreases considerably. At mobility ratios less than 1, the minimum point and as it decreases the mobility ratio decreases, the distance between the curves for the same conductivity increases.

Figure 4 shows pressure derivative behaviors for finite-conductivity faulty systems under fault skin factor conditions and mobility ratios. As expected, the skin creates additional resistance to flow within the fault plane for some period of time, resembling a situation similar to a sealing fault for all conductivity values. The mobility ratio only affects the minimum point in the pressure derivative.

If the dimensionless fault conductivity is assumed to be zero and the hydraulic diffusivity is also set to zero, essentially there is no fault and the solution degenerates to that of a single composite system as presented by Bixel et al. [5]. Additionally to these conditions, if the mobility ratio is assumed to be infinite, reservoir zone 2 provides a strong pressure support to reservoir zone 1. Then, the behavior looks like the case of a well near a constant-pressure boundary. Other limitations of the model are provided by Anisur Raman et al. [11].

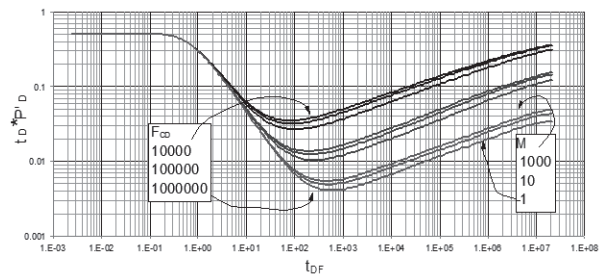


Figure 2. Effect of mobility ratio on pressure derivative dimensionless. $s_F = 0$ y $M > 1$

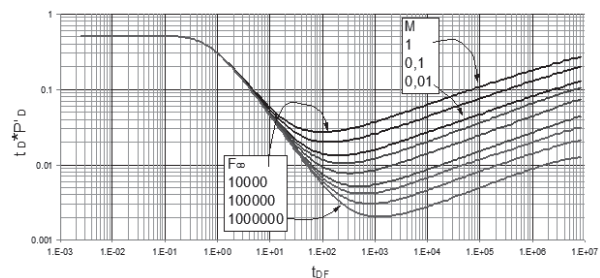


Figure 3. Effect of mobility ratio on pressure derivative dimensionless. $s_F = 0$ y $M < 1$

2. MATHEMATICAL FORMULATION

The dimensionless quantities used in this work are defined as:

$$P_D = \frac{k_1 h}{141.2 q \mu B} \Delta P \quad (1)$$

$$t_D * P_D = \frac{k_1 h (t * \Delta P')}{141.2 q \mu B} \quad (2)$$

$$t_{DF} = \frac{0.0002637 k_1 t}{\phi \mu c_i L_F^2} \quad (3)$$

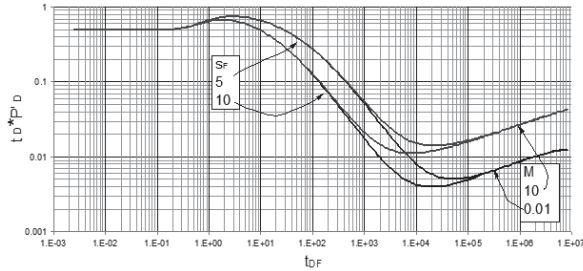


Figure 4. Effect of fault skin factor and mobility ratio on pressure derivative dimensionless, $h_D = 1$

$$h_D = \frac{h}{L_F} \quad (4)$$

$$F_{CD} = \frac{k_f w_f}{k_1 L_F} \quad (5)$$

$$M = \frac{k_2}{k_1} \quad (6)$$

The formulation of the equations follows the philosophy of the *TDS* Technique [13]. It means, several specific regions and “fingerprints” found on the pressure and pressure derivative behavior are dealt with:

1) The permeability and skin factors are found using the following equations, Tiab (1993):

$$k = \frac{70.6 q \mu B}{h (t * \Delta P')_r} \quad (7)$$

$$s = \frac{1}{2} \left(\frac{\Delta P_r}{(t * \Delta P')_r} - \ln \left(\frac{k t_r}{\phi \mu c_i r_w^2} \right) + 7.43 \right) \quad (8)$$

2) According to figures 2-4, the early radial flow ends at:

$$t_{DFer} = 0.25 \quad (9)$$

Plugging *Equation 3* into the above expression and solving for the distance from the well to the fault:

$$L_F = 0.0325 \sqrt{\frac{k t_{er}}{\phi \mu c_i}} \quad (10)$$

3) The governing dimensionless pressure derivative for the steady-state flow caused by the fault is:

$$(t_D * P_D')_{ss} = \frac{1}{2} (1 + s_F h_D)^2 \frac{1}{t_{DF}} \quad (11)$$

Equation 11 is a corrected form of an expression introduced by Abbaszadeh and Cinco-Ley [10] and considers the dimensionless pay thickness.

Replacing the dimensionless quantities given by *Equations 2, 3 and 4* into *Equation 11* and solving for the fault skin factor will result:

$$s_F = \frac{L_F}{h} \left[\sqrt{\left(\frac{3.7351 \times 10^{-6} k^2 h t_{ss} (t * \Delta P')_{ss}}{q \mu^2 B \phi c_i L_F^2} \right)} - 1 \right] \quad (12)$$

4) The pressure and pressure derivative dimensionless expressions for the bilinear-flow regime, given by Abbaszadeh and Cinco-Ley [10] and corrected here are:

$$P_D = \frac{2.6084}{\sqrt{F_{CD} \frac{\sqrt{M} + 1}{2\sqrt{M}}}} \sqrt[4]{t_{DF}} + s_{BL} \quad (13)$$

$$t_D * P_D' = \frac{0.6521}{\sqrt{F_{CD} \frac{\sqrt{M} + 1}{2\sqrt{M}}}} \sqrt[4]{t_{DF}} \quad (14)$$

Replacing the dimensionless quantities given by *Equations 2, 3 and 5* into *Equation 14* will result in an expression to estimate effective fault conductivity using any arbitrary point on the pressure derivative during the bilinear-flow regime;

$$(k_f w_f)_{eff} = k_f w_f \frac{\sqrt{M} + 1}{2\sqrt{M}} = 137.67 \left(\frac{q \mu B}{h (t * \Delta P')_{BL}} \right)^2 \sqrt{\frac{t_{BL}}{\phi \mu c_i k}} \quad (15)$$

5) Using the minimum pressure derivative coordinate, correlating with the fault skin factor and the dimensionless pay thickness, we obtain with a non-linear regression process another expression for the effective fault conductivity:

$$\sqrt{F_{CD\text{eff}}} = \sqrt{F_{CD} \frac{\sqrt{M}+1}{2\sqrt{M}}} = \frac{a+c(t_D * P_D')_{\min}}{1+b(t_D * P_D')_{\min}+d(t_D * P_D')_{\min}^2} \sqrt{(1+S_F h_D)} \quad (16)$$

Replacing the dimensionless quantities:

$$(k_f w_f)_{\text{eff}} = k_f w_f \frac{\sqrt{M}+1}{2\sqrt{M}} = k L_F \left(\frac{a+c(t_D * P_D')_{\min}}{1+b(t_D * P_D')_{\min}+d(t_D * P_D')_{\min}^2} \right)^2 \left(1+S_F \frac{h}{L_F} \right) \quad (17)$$

Where the constants are $a = -14048.04$, $b = -3044.648$, $c = -513947.31$ and $d = -279062.51$

6) With the effective fault conductivity and through an iterative procedure, assuming a value of dimensionless conductivity, we find the mobility ratio:

$$F_{CD} = \frac{a+c*\ln(X)+e*\ln(Y)+g*(\ln(X))^2+i*(\ln(Y))^2+k*\ln(X)*\ln(Y)}{1+b*\ln(X)+d*\ln(Y)+f*(\ln(X))^2+h*(\ln(Y))^2+j*\ln(X)*\ln(Y)} \quad (18)$$

Where:

$$X = \frac{\sqrt{M}+1}{2(1+0.84S_F h_D)\sqrt{M}} = \frac{F_{CD\text{eff}}}{F_{CD}(1+0.84S_F h_D)} \quad (19)$$

$$Y = F_{CD} * (t_D * P_D')_{\min} \quad (20)$$

Where the constants are: $a = -149853.12$, $b = -0.09009733$, $c = 19693.58889$, $d = -0.22773859$, $e = 47430.36913$, $f = 0.001902798$, $g = -701.266695$, $h = 0.012815243$, $i = -3646.98008$, $j = -0.010110749$ and $k = -3024.39415$

7) The dimensionless pressure derivative lines obtained from the early radial flow ($t_D * P_D' = 0.5$) and the steady-state flow regimes (equation 11) intercepts at:

$$0.5 = \frac{1}{2} (1+S_F h_D)^2 \frac{1}{t_{DF}} \quad (21)$$

$$t_{DF\text{rssi}} = (1+S_F h_D)^2 \quad (22)$$

Replacing the dimensionless time into Equation 22 and solving for the well distance to the fault will result in:

$$L_F = \sqrt{\frac{0.0002637 k t_{\text{rssi}}}{\phi \mu c_i}} - S_F h \quad (23)$$

8) The line corresponding to the steady state and the bilinear flow line of the dimensionless pressure derivative intersect at (equations 11 and 14):

$$\frac{0.6125}{\sqrt{F_{CD} \frac{\sqrt{M}+1}{2\sqrt{M}}}} t_{DF}^{0.25} = \frac{1}{2} (1+S_F h_D)^2 \frac{1}{t_{DF}} \quad (24)$$

$$t_{DF\text{ssBli}} = \left[\frac{(1+S_F h_D)^2 \sqrt{F_{CD} \frac{\sqrt{M}+1}{2\sqrt{M}}}}{1.3042} \right]^{0.8} \quad (25)$$

Replacing the dimensionless time defined by Equation 3 into Equation 25 and solving for the effective conductivity fault will result in:

$$k_f w_f \frac{\sqrt{M}+1}{2\sqrt{M}} = 1.9207 \times 10^{-9} k L_F \left(\frac{k t_{\text{ssBli}}}{\phi \mu c_i L_F^2} \right)^{2.5} 1 / \left(1+S_F \frac{h}{L_F} \right)^4 \quad (26)$$

9) If the dimensionless effective fault conductivity is bigger than 2.5×10^8 , the bilinear flow disappears and the linear flow appears exhibiting a $1/2$ -slope straight line on the pressure derivative curve. In this case we have an infinite-conductivity fault. The dimensionless pressure derivative expression for the above mentioned linear flow regime is:

$$t_D * P_D' = \frac{5.6 \times 10^{-6} \sqrt{M}}{\sqrt{M}+1} \sqrt{t_{DF}} \quad (27)$$

Replacing the dimensionless quantities given by Equations 2 and 3 into Equation 27 will result in another expression useful to estimate the distance from the well to the fault;

$$L_F = 1.284 \times 10^{-5} \frac{\sqrt{M}}{\sqrt{M}+1} \frac{qB}{h(t * \Delta P')_L} \sqrt{\frac{\mu t_L}{k \phi c_i}} \quad (28)$$

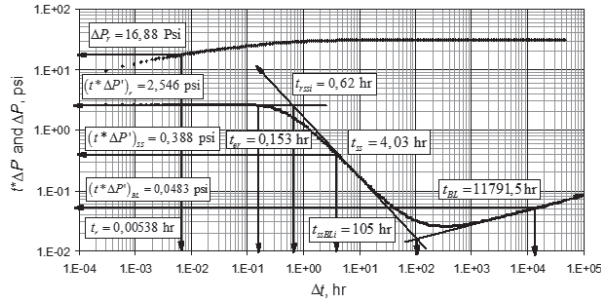


Figure 5. Pressure and Pressure derivative for example 1

3. EXAMPLES

3.1 EXAMPLE 1

A pressure test synthetic generated using a commercial software of a well inside an infinite reservoir was generated with the data given in Table 1. Pressure and pressure derivative data are reported in Figure 5. It is required to estimate permeability, skin factor formation, distance to fault, fault conductivity and mobility ratio.

Solution. The log-log plot of pressure and pressure derivative against production time is given in Figure 5 from which the following information was read:

$$\begin{aligned}
 t_r &= 0.00538 \text{ hr} & \Delta P_r &= 16.88 \text{ psi} & (t^* \Delta P)_r &= 2.546 \text{ psi} \\
 t_{er} &= 0.153 \text{ hr} & t_{ss} &= 4.02 \text{ hr} & (t^* \Delta P)_{ss} &= 0.386 \text{ psi} \\
 t_{BL} &= 11791.5 \text{ hr} & (t^* \Delta P)_{BL} &= 0.0483 \text{ psi} & t_{rssi} &= 0.62 \text{ hr} \\
 t_{ssBLi} &= 105 \text{ hr} & (t^* \Delta P)_{min} &= 0.02499 \text{ psi} & &
 \end{aligned}$$

First, the formation permeability is evaluated with Equation 7 and the skin factor with Equation 8:

$$k = \frac{70.6 * 300 * 0.7747 * 1.553}{100 * 2.546} = 100.086 \text{ md}$$

$$s = \frac{1}{2} \left(\frac{16.88}{2.546} - \ln \left(\frac{100.086 * 0.00538}{0.15 * 0.7747 * 1.4576 * 10^{-5} * 0.5^2} \right) + 7.43 \right) = 0.00211$$

The distance to fault is evaluated with Equation 10 and the fault skin factor with Equation 12:

$$L_F = 0.0325 \sqrt{\frac{100.086 * 0.153}{0.15 * 0.7747 * 1.4576 * 10^{-5}}} = 97.72 \text{ ft}$$

$$s_F = \frac{97.72}{100} \left[\sqrt{\frac{3.7351 * 10^{-5} * 100.086^2 * 100 * 4.03 * 0.388}{300 * 0.7747^2 * 1.553 * 0.15 * 1.4576 * 10^{-5} * 97.72^2}} - 1 \right] = 0.00105$$

The distance to fault is re-estimated with Equation 23:

$$L_F = \sqrt{\frac{0.0002637 * 100.086 * 0.62}{0.15 * 0.7747 * 1.4576 * 10^{-5}} - 0.00105 * 100} = 98.18 \text{ ft}$$

The effective fault conductivity is evaluated with Equation 15 and re-estimated with Equations 17 and 26:

$$k_f w_f \frac{\sqrt{M} + 1}{2\sqrt{M}} = 137.67 \left(\frac{300 * 0.7747 * 1.553}{100 * 0.0483} \right)^2 \left(\frac{11791.5}{100.086 * 0.15 * 0.7747 * 1.4576 * 10^{-5}} \right)^{0.5} = 6.411 * 10^9 \text{ md-ft}$$

$$(t_D * P_D')_{min} = \frac{100.086 * 100 * 0.02499}{141.2 * 300 * 0.7747 * 1.553} = 0.004908$$

$$k_f w_f \frac{\sqrt{M} + 1}{2\sqrt{M}} = 100.086 * 97.72 \left(\frac{a + c * 0.004908}{1 + b * 0.004908 + d * 0.004908^2} \right)^2 \left(1 + 0.00105 * \frac{100}{97.72} \right)$$

$$k_f w_f \frac{\sqrt{M} + 1}{2\sqrt{M}} = 6.295 * 10^9 \text{ md-ft}$$

$$k_f w_f \frac{\sqrt{M} + 1}{2\sqrt{M}} = 1.9207 * 10^{-9} * 100.086 * 97.72 \left(\frac{100.086 * 105}{0.15 * 0.7747 * 1.4576 * 10^{-5} * 97.72^2} \right)^{2.5} \left[\frac{1}{1 + 0.00105 * \frac{100}{97.72}} \right]^4$$

$$k_f w_f \frac{\sqrt{M} + 1}{2\sqrt{M}} = 6.365 * 10^9 \text{ md-ft}$$

Averaging the above values, the effective dimensionless fault conductivity is:

$$F_{CD} \frac{\sqrt{M} + 1}{2\sqrt{M}} = \frac{6.357 * 10^9}{100.086 * 97.72} = 649973.16$$

Applying Equation 18 and by iterative procedure, the dimensionless fault conductivity and the mobility ratio are:

$$F_{CD} = 999671.676$$

$$M = 11.08$$

Finally, the fault conductivity is:

$$k_f w_f = 9.777 \times 10^9 \text{ md-ft}$$

3.2 EXAMPLE 2

Another synthetic pressure test pressure of a well inside an infinite reservoir was generated with the data given in Table 1. Pressure and pressure derivative data are reported in Figure 6. It is required to estimate permeability, skin factor formation, distance to fault and fault conductivity.

Solution. The log-log plot of pressure and pressure derivative against production time is given in Figure 6 from which the following information was read:

$$\begin{aligned} t_r &= 0.01152 \text{ hr} & \Delta P_r &= 22.05 \text{ psi} & (t^* \Delta P^*)_r &= 2.83 \text{ psi} \\ t_{er} &= 0.11 \text{ hr} & t_{ss} &= 39.35 \text{ hr} & (t^* \Delta P^*)_{ss} &= 0.128 \text{ psi} \\ t_{BL} &= 20077.8 \text{ hr} & (t^* \Delta P^*)_{BL} &= 0.0346 \text{ psi} & t_{rsi} &= 1.85 \text{ hr} \\ t_{ssBLi} &= 390 \text{ hr} & (t^* \Delta P^*)_{min} &= 0.02091 \text{ psi} \end{aligned}$$

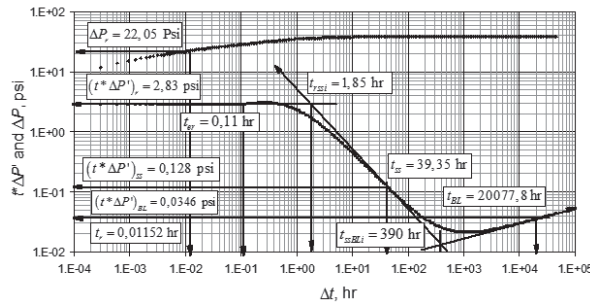


Figure 6. Pressure and Pressure derivative for example 2

Table 1. Reservoir and fluid data for examples

PARAMETER	EXAMPLE 1	EXAMPLE 2
q (bbl/D)	300	250
B (rb/STB)	1.553	1.553
μ (cp)	0.7747	0.7747
h (ft)	100	50
r_w (ft)	0.5	0.5
ϕ	0.15	0.15
c_t (1/psi)	1.4576×10^{-5}	1.4576×10^{-5}
k_1 (md)	100	150
k_2 (md)	1200	10
L_F (ft)	100	100
F_{CD}	1000000	1000000
s_F	0	2

First, the formation permeability is evaluated with Equation 6 and the skin factor with Equation 7 giving value of 150.07 md and 0.00037, respectively.

A values of 101.46 ft is found with Equation 10 for the distance from the wellbore to the fault. A fault skin factor of 2.05 is estimated with Equation 12. Another value of distance from the wellbore to the fault calculated with Equation 23 results to be 105.4 ft.

The effective fault conductivity is evaluated with Equation 15 and re-estimated with Equations 17 and 26. The respective values are 3.698×10^{10} , 3.943×10^{10} and 3.697×10^{10} md-ft.

Averaging the above values the effective dimensionless fault conductivity, is 2481922.13. Applying Equation 18 and by iterative procedure, the dimensionless fault conductivity and the mobility ratio are 998166.45 and 0.0633. Finally the fault conductivity is 1.524×10^{10} md-ft.

CONCLUSIONS

Pressure derivative behavior for a well located near finite-conductivity fault with contrast of mobilities was studied and an expression to estimate the mobility ratio was introduced.

The expressions for to estimate the distance from the well to the fault, fault conductivity and fault skin factor, when the mobility ratio is unity were corrected for introducing the contrast effect mobilities.

There is a need of running a test for a very long time to observe the second radial flow corresponding to the zone in the other side of the fault. The bilinear flow regime is used obtain an effective conductivity fault.

ACKNOWLEDGMENTS

The authors gratefully thank Universidad Surcolombiana for providing support to the completion of this work.

REFERENCES

- TROCCHIO, J.T. Investigation on Fateh Mishrif – Fluid Conductive Faults. Journal of Petroleum Technology. 1990, vol 42, num 2, p.1038-1045.
- CINCO-LEY, L.H., SAMANIEGO, F.V., & DOMÍNGUEZ, A.N. Unsteady State Flow Behavior

- for a Well near a Natural Fracture. *SPE Annual Technical Conference and Exhibition*, New Orleans, USA. SPE 6019, 1976.
3. STEWART, G., GUPTA, A., and WESTAWAY, P. The Interpretation of Interference Tests in a Reservoir with a Sealing and Partially Communicating Faults. SPE European Offshore Petroleum Conference, London. SPE 12967, 1984.
 4. YAXELY, L.M. Effect of Partially Communicating Fault on Transient Pressure Behavior. SPE Formation Evaluation. 1987, vol 2, num 4, p. 590-598.
 5. BIXEL, H.C., LARKIN, B.K., & VAN POOLEN, H.K. Effect of linear Discontinuities on Pressure Buildup and Drawdown Behavior. *Journal of Petroleum Technology*. 1963, vol 15, num 8, p.885-895.
 6. AMBASTHA, A.K., McLEROY, P.G., & GRADER, A.S. Effects of a Partially Communicating Fault in a Composite Reservoir on Transient Pressure Testing. *SPE Formation Evaluation*. 1989, vol 4, num 2, p. 210-218.
 7. VAN EVERDINGEN, A.F. The Skin Effect and Its Influence on the Productivity Capacity of a Well. *Journal of Petroleum Technology*. 1953, vol 5, num 6, p. 171-176.
 8. HURST, W. (1953). Establishment of the Skin Effect and Its Impediment to Fluid Flow into a Wellbore. *Petroleum Engineering*. 1953, vol 25. B6-B16
 9. BOUSSILA, A.K., TIAB, D. & OWAYED, J. Pressure Behavior of Well near a Leaky Boundary in Heterogeneous Reservoirs. *SPE Production and Operations Symposium*, Oklahoma City, Oklahoma, USA. SPE 80911. 2003.
 10. ABBASZADEH, M.D. & CINCO-LEY, H. (1995). Pressure-Transient Behavior in a Reservoir with a Finite Conductivity Fault. SPE Formation Evaluation. 1995, vol 10, num 3, p. 26-32.
 11. ANISUR RAHMAN, N.M., MILLER, M.D. & MATTAR, L. Analytical Solution to the Transient-Flow Problems for a Well Located near a Finite-Conductivity Fault in Composite Reservoirs. SPE Annual Technical Conference and Exhibition, Denver, Colorado, USA. SPE 84295. 2003.
 12. ESCOBAR, F.H., MARTÍNEZ, J.A. & MONTEALEGRE-MADERO, M. Pressure Transient analysis for a reservoir with a finite-conductivity fault. *CT&F – Ciencia, Tecnología y Futuro*. 2013, vol 5, num 2, p.5-18.
 13. TIAB, D. Analysis of Pressure and Pressure Derivative without Type-Curve Matching: 1- Skin and Wellbore Storage. *Journal of Petroleum Science and Engineering*. 1993, vol 12, p.171-181.

NOMENCLATURE

B	Oil formation factor, rb/STB
c_i	Total system compressibility, 1/psi
F_{CD}	Dimensionless fault conductivity
h	Formation thickness, ft
h_D	Dimensionless pay thickness
k	Permeability, md
k_{JW_f}	Fault conductivity, md-ft
L_F	Distance from the well to the fault, ft
M	Mobility ratio
m	Slope
q	Flow rate, STB/D
r	Radius, ft
s	Skin factor
s_F	Fault skin factor
s_{BL}	Bilinear flow skin factor
t	Time, hr
$t^*\Delta P'$	Pressure derivative, psi

GREEKS

D	Change, drop
f	Porosity, Fraction
m	Viscosity, cp

SUFFICES

BL	Bilinear flow
D	Dimensionless
eBL	End of bilinear flow
$eBLD$	End of bilinear flow, dimensionless
er	End of radial flow
F	Fault
i	Intersection

<i>min</i>	Minimum	<i>ss</i>	Steady state
<i>r</i>	Radial	<i>ssBLi</i>	Steady state and bilinear intersection
<i>rsi</i>	Radial and steady state intersection	<i>w</i>	Wellbore

Recepción: 17 de Junio de 2013
Aceptación: 19 de Diciembre de 2013